MMSE Subchannel Decision Feedback Equalization for Filter Bank Based Multicarrier Systems

Leonardo G. Baltar, Dirk S. Waldhauser and Josef A. Nossek
Institute for Circuit Theory and Signal Processing
Technische Universität München
Arcisstr. 21, 80290 München, Germany
Email: {leo.baltar, waldhauser, josef.a.nossek}@tum.de

***Abstract*— In this work we present a per-subchannel nonlinear equalizer for a class of filter bank based multicarrier (FBMC) systems. We consider the class of exponentially modulated FBMCs with offset quadrature amplitude modulated (OQAM) input symbols. We design a fractionally spaced decision feedback equalizer (DFE) that minimizes the mean squared error (MMSE) and takes into account the inter-(sub)channel interference (ICI). The input of each equalizer comprises only the output of each subchannel. In the simulation results we show that, despite its increased computational complexity, the performance and the higher bandwidth efficiency of OQAM FBMC systems makes them a competitive alternative to conventional multicarrier systems like cyclic prefix based orthogonal frequency division multiplexing (CP-OFDM).**

I. Introduction

The advantages of using multicarrier (MC) modulation in broadband wired and wireless communication systems is widely known. The idea to divide the frequency spectrum into many narrow subchannels is not new, but only in the last decade a widespread use in practical systems could be observed. There are many classes of MC systems, but the CP-OFDM is certainly the most investigated. It offers the advantage of efficient and simple implementation and trivial channel equalization. Because of the insertion of redundancy (CP), only one tap per subchannel is necessary to compensate the frequency selectivity of the channel. Drawbacks of using CP-OFDM include a loss in spectral efficiency, because some redundancy is inserted, a higher level of out-of-band radiation, since the subcarriers pulse-shaping is trivial, and a higher sensibility to narrowband interferers, because the low attenuation of the sidelobes implies an undesired overlap of the subchannels.

CP-OFDM is based on the general MC concept of transmultiplexers, which are composed of exponentially modulated analysis and synthesis filter banks, also called FBMC systems. Of particular interest are the maximally decimated filter banks. Instead of using a rectangular window for shaping the pulses a finite impulse response (FIR) prototype filter that has longer impulse response than the symbol period, i.e. the number of filter coefficients is higher than the number of subchannels M, is modulated by complex exponentials and employed in each subchannel. As a consequence, the latter can be more concentrated in frequency and only the overlap of immediately adjacent subchannels is significant. But it is known from filter banks and communications theory [1] that the real and imaginary part of the inputs of such a system have to be staggered, resulting in OQAM signals.

The equalization problem in FBMC systems is still an area of active research. We focus here on solutions that depend only on the outputs of each subchannel. In this way per-subchannel equalizers work like single carrier (SC) equalizers for OQAM modulated symbols, but with the difference that ICI is present. Since noise cannot be considered white at the output of a filter with bandwidth smaller than the sampling frequency, we have to consider it in the equalizer design.

From communications theory [2] it is known that the optimal receiver for a frequency selective (band limited) channel with band limited transmit signal and additive white Gaussian noise (AWGN) is composed by a (analog) matched filter (MF), a sampling device (at symbol rate) and a maximum likelihood sequence estimator (MLSE). But the latter is usually impractical in terms of complexity. Two practical sub-optimum solutions with lower computational burden are the linear equalizer (LE) and the DFE that work at symbol rate.

An analog filter matched to the transfer function formed by the transmitter filter and the transmission channel is not easy to be designed (e.g. due to channel variations and the difficult estimation). Alternatively, the receive filter is designed to match the transmitted signal, and is followed by a fractionally spaced equalizer (FSE).

In an FBMC system with OQAM input symbols the equalizer can be inserted before the de-staggering, leading to an FSE working at $2/T$, where $1/T$ is the symbol rate.

In [3] the author has presented a first solution to the equalization problem in an OQAM FBMC system. The coefficients of the linear MMSE FSE have been calculated iteratively using a steepest descent method and no closed form solution is given. In [4] both a linear equalizer and DFE for a general class of FBMCs have been presented, but they use the output of many subcarriers to feed the equalizer. The authors of [5] have extended the solution of [3] to the DFE case using three feedback filters for each subchannel. The authors of [6] have proposed some solutions for the LE for another class of exponentially modulated FBMC systems. The solution is based on the minimization of the MSE in the frequency domain instead of minimizing the ISI directly. Some analytical solutions have been given, but the choice of the number of coefficients is limited to three. In a recent work [7] we have derived a closed formula for the linear per-subchannel FSE according to the MMSE criterion for a class of OQAM FBMC systems.

In this paper we have extended the results presented in [7] and have computed the optimum (according the MMSE criterion) coefficients of the per-subchannel fractionally spaced DFE for an OQAM based FBMC system. Our solution takes into account the ICI and the noise correlations introduced by the receive filters.

A. Notation

We employ the following notation throughout this work: The real and imaginary parts of a signal, an impulse response or a matrix are written as $\mathrm{Re}[(\bullet)]=(\bullet)^{(\mathrm{R})}$ and $\mathrm{Im}[(\bullet)]=(\bullet)^{(\mathrm{I})}$, viz. $(\bullet)=(\bullet)^{(\mathrm{R})}+\mathrm{j}\,(\bullet)^{(\mathrm{I})}$, with $\mathrm{j}=\sqrt{-1}$. Vectors with a time index $n\in\mathbb{Z}$ are always a stack of signal samples, e.g. $\boldsymbol{x}[n]=\big[x[n],x[n-1],\ldots,x[n-N]\big]^{\mathrm{T}}\in\mathbb{C}^{N+1}$, where N is explicitly given each time. $\boldsymbol{I}_N$ denotes the $N\times N$ identity matrix. $\mathbf{0}_M$, $\mathbf{0}_{M\times N}$ and $\boldsymbol{e}_\nu$ represent an M-dimensional zero

vector, an $M \times N$ zero matrix and a vector with a 1 in the ν-th position and all the other elements equal to zero.

II. OQAM FBMC SYSTEM STRUCTURE

A general FBMC system overview is given in Fig. 1. The transmitter is usually called the synthesis filter bank (SFB) and the receiver the analysis filter bank (AFB). We assume that the complex input symbols $d_k[m]$ are QAM modulated, independent and identically distributed.

In the SFB the real and imaginary parts of each complex inputs $d_k[n]$ are staggered as shown in Fig. 2 generating OQAM signals $x'_k[n]$ at the double symbol rate. Those signals are upsampled by $M/2$ and fed into the transmitter subfilters, that are defined as

$$h_k[l] = h_0[l] \exp\left(\mathrm{j}\, 2\pi kl/M\right), \quad l = -KM/2, \ldots, KM/2, \quad (1)$$

where $h_0[l]$ is called the prototype filter and has length $KM+1$. It is worth noting that the exponential modulation of the prototype filter can be implemented efficiently using the polyphase decomposition and the fast Fourier transform (FFT) (e.g., see [8]).

After the subfilters, all the signals are added up, forwarded to the radio frequency (RF) processing and transmitted. At the receiver after the RF processing the signal is filtered again and downsampled (cf. Fig. 3). The downsampled signal is equalized and then the OQAM samples are de-staggered. As we will show in the next section, the de-staggering is a building block of the DFE structure.

It is worth mentioning that the impulse response $h_{\mathrm{ch}}[l]$ in Fig. 3 encompasses the whole processing between the SFB and the AFB and the multipath propagation channel.

III. MMSE PER-SUBCHANNEL DFE

We consider here an FBMC system where only adjacent subchannel filters overlap significantly, i.e. the interference of non-adjacent subchannels is negligible, assuming that the prototype filter has a high attenuation level in the stop-band. That is usually true for $K \geq 4$. Thus, the received vector $\boldsymbol{y}_k[n] \in \mathbb{C}^N$ containing the samples of the received signal before the OQAM de-staggering can be approximated by

$$\boldsymbol{y}_k[n] \approx \boldsymbol{G}'_k \boldsymbol{x}'_k[n] + \boldsymbol{M}'_k \boldsymbol{x}'_{k-1}[n] + \boldsymbol{N}'_k \boldsymbol{x}'_{k+1}[n] + \boldsymbol{\Gamma}_k \boldsymbol{\eta}[l], \quad (2)$$

where $\boldsymbol{G}'_k$, $\boldsymbol{M}'_k$ and $\boldsymbol{N}'_k \in \mathbb{C}^{N\times(L+1)}$ are the corresponding convolution matrices belonging to the impulse responses $g'_k[n]$, $m'_k[n]$ and $n'_k[n]$ as exhibited in Fig. 3. We assume that those impulse responses have length Q giving $L = N+Q-2$. Note that $g'_k[n]$ is the impulse response from the input to the output of the actual subchannel and $m'_k[n]$ and $n'_k[n]$ are the impulse responses from the inputs of the adjacent subchannels to the output of the actual subchannel. The matrix $\boldsymbol{\Gamma}_k$ comprises the filtering of the white Gaussian noise $\eta[l]$ with $h_k[l]$ and the downsampling by $M/2$. $\boldsymbol{\Gamma}_k$ inserts correlation in the noise samples transforming it into colored noise.

The vector $\boldsymbol{x}'_k[n] \in \mathbb{C}^{L+1}$, i.e. with the samples of the signal after the staggering in Fig. 2 and before the upsampling in Fig. 3, can be written as

$$\boldsymbol{x}'_k[n] = \begin{cases} \left[a_k[m],\, \mathrm{j}\, b_k[m],\, a_k[m-1],\, \ldots, x'_k[n-L]\right]^{\mathrm{T}}, & k \text{ even}, \\ \left[\mathrm{j}\, b_k[m],\, a_k[m],\, \mathrm{j}\, b_k[m-1],\, \ldots, x'_k[n-L]\right]^{\mathrm{T}}, & k \text{ odd}, \end{cases} \quad (3)$$

where $n = 2m$, $m \in \mathbb{Z}$ and the last element $x'_k[n-L]$ depends on L and k according to Table I.

The structure of the proposed DFE for even indexed subchannels is shown in Fig. 4. In the case of odd indexed subchannels the delay elements are moved to the opposite branch resulting in an exchange

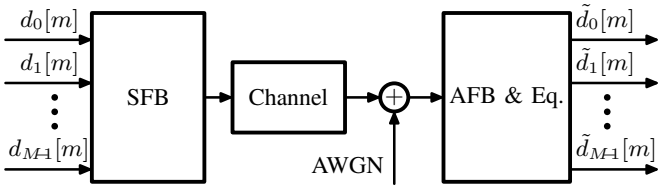

Fig. 1. FBMC System Overview

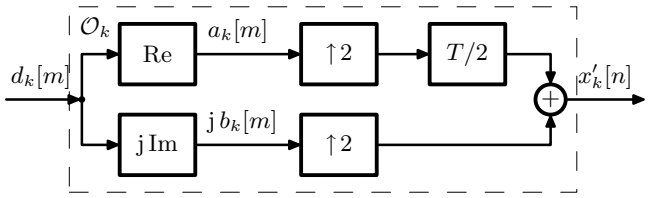

Fig. 2. OQAM Staggering $\mathcal{O}_k$, k even

TABLE I
LAST ELEMENT OF VECTOR $\boldsymbol{x}'_k[n]$

$x'_k[n-L]$	L even	L odd
k even	$a_k[m-\lfloor L/2 \rfloor]$	$\mathrm{j}\, b_k[m-\lfloor L/2 \rfloor]$
k odd	$\mathrm{j}\, b_k[m-\lfloor L/2 \rfloor]$	$a_k[m-\lfloor L/2 \rfloor]$

of the roles of real and imaginary parts in time. The output of the downsampling $y_k[n]$ is then filtered by the subcarrier feedforward filter $w_k[n]$ of length N. From this signal the output of the feedback filter $f_k[n]$ of length $B+1$ is subtracted. The resulting signal is fed into the de-interleaver $\mathcal{O}'_k$ and finally the symbols are detected in a decision device. The detected symbols are then used by the feedback filter.

If we assume that the received symbols are correctly detected, the input of the feedback filter $\hat{\boldsymbol{x}}_k[n] \in \mathbb{R}^{B+1}$ can be defined as

$$\hat{\boldsymbol{x}}_k[n] = \begin{cases} \big[a_k[m-\nu-1],\, b_k[m-\nu-1],\, a_k[m-\nu-2], \\ \qquad \ldots, \hat{x}_k[n-2\nu-B]\big]^{\mathrm{T}}, & k \text{ even}, \\ \big[b_k[m-\nu-1],\, a_k[m-\nu-2],\, b_k[m-\nu-2], \\ \qquad \ldots, \hat{x}_k[n-2\nu-B]\big]^{\mathrm{T}}, & k \text{ odd}, \end{cases} \quad (4)$$

where the last element $\hat{x}_k[n-2\nu-B]$ depends on B and k according to Table II.

TABLE II
LAST ELEMENT OF VECTOR $\hat{\boldsymbol{x}}_k[n]$

$\hat{x}_k[n-2\nu-B]$	B even	B odd
k even	$b_k[m-\nu-\lfloor B/2 \rfloor]$	$a_k[m-\nu-\lfloor B/2 \rfloor]$
k odd	$a_k[m-\nu-\lfloor B/2 \rfloor]$	$b_k[m-\nu-\lfloor B/2 \rfloor]$

The estimation of the real and the imaginary parts of the transmitted symbol after the equalization is given by

$$\begin{aligned} \hat{a}_k[m] &= \mathrm{Re}\left[\boldsymbol{w}_k^{\mathrm{H}} \boldsymbol{y}_k[n] - \boldsymbol{f}_k^{\mathrm{H}} \hat{\boldsymbol{x}}_k[n]\right] \\ &= \boldsymbol{w}_k^{(\mathrm{R}),\mathrm{T}} \boldsymbol{y}_k^{(\mathrm{R})}[n] + \boldsymbol{w}_k^{(\mathrm{I}),\mathrm{T}} \boldsymbol{y}_k^{(\mathrm{I})}[n] - \boldsymbol{f}_k^{(\mathrm{R}),\mathrm{T}} \hat{\boldsymbol{x}}_k[n], \end{aligned} \quad (5)$$

$$\begin{aligned} \hat{b}_k[m] &= \mathrm{Im}\left[\boldsymbol{w}_k^{\mathrm{H}} \boldsymbol{y}_k[n-1] - \boldsymbol{f}_k^{\mathrm{H}} \hat{\boldsymbol{x}}_k[n-1]\right] \\ &= \boldsymbol{w}_k^{(\mathrm{R}),\mathrm{T}} \boldsymbol{y}_k^{(\mathrm{I})}[n-1] - \boldsymbol{w}_k^{(\mathrm{I}),\mathrm{T}} \boldsymbol{y}_k^{(\mathrm{R})}[n-1] - \boldsymbol{f}_k^{(\mathrm{I}),\mathrm{T}} \hat{\boldsymbol{x}}_k[n-1]. \end{aligned} \quad (6)$$

Fig. 5 shows an example of a desired impulse response after the equalization and before the downsampling by two when no residual ISI is present. Except for the sample with amplitude one, all the others

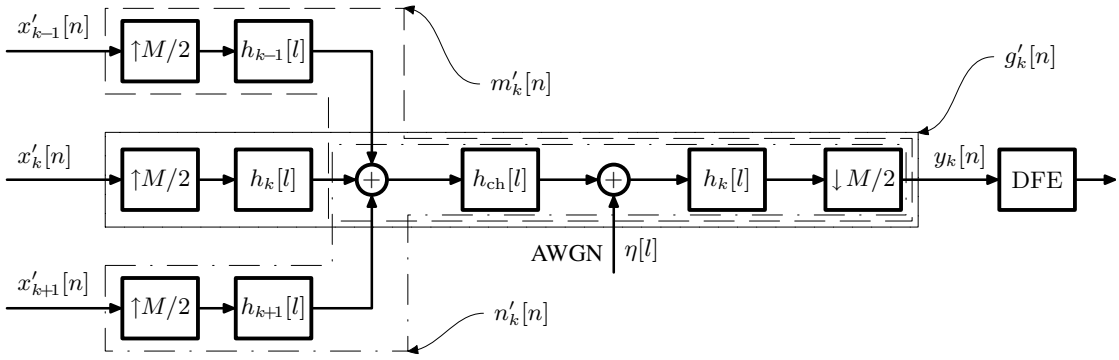

Fig. 3. Subchannel Model for the FBMC System

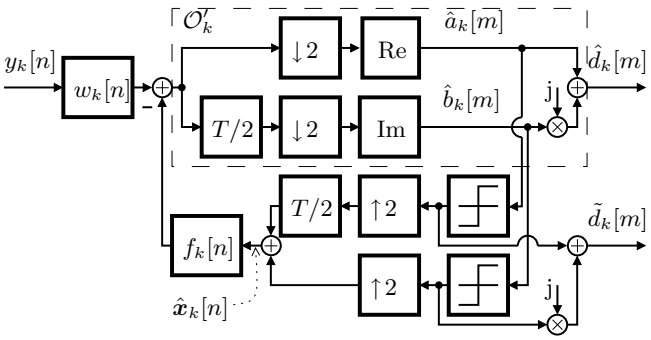

Fig. 4. Per-subchannel DFE and OQAM de-staggering $\mathcal{O}'_k$, k even

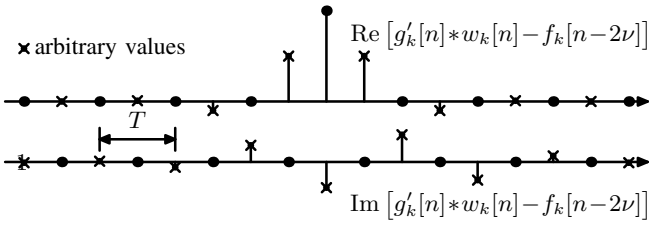

Fig. 5. Desired OQAM impulse response

with filled circles have value zero, whereas those with an x-mark are allowed to have any value (don't cares).

Our design criterion is the MMSE between the estimated signal $\hat{d}_k[m] = \hat{a}_k[m] + \mathrm{j}\,\hat{b}_k[m]$ and the input signal $d_k[m] = a_k[m] + \mathrm{j}\,b_k[m]$. But if $a_k[m]$ and $b_k[m]$ are wide-sense stationary and uncorrelated, i.e. $\mathrm{E}\left[a_k[m]b_k[m+m']\right] = 0, \forall m' \in \mathbb{Z}$, we can decompose the error into its real and imaginary part. The optimization problem for the real part can expressed by

$$(\boldsymbol{w}_{k,\mathrm{o}}, \boldsymbol{f}_{k,\mathrm{o}}) = \arg \min_{(\boldsymbol{w}_k, \boldsymbol{f}_k)} \mathrm{E}\left[|\hat{a}_k[m] - a_k[m-\nu]|^2\right], \tag{7}$$

where the delay ν depends on the prototype filter, the equalizer and the propagation channel lengths and can be optimized for minimizing the MSE. Because we have not dealt with the optimization of that delay, we have used a fixed value for it throughout the simulations.

Both $\hat{a}_k[m]$ and $\hat{b}_k[m]$ are functions of the feedforward filter coefficients $w_{k,n}$, but from (5) and (6) it is clear that, in order to obtain $\hat{a}_k[m]$, only the real part of the feedback filter $f^{(\mathrm{R})}_{k,n}$ is relevant, and to obtain $\hat{b}_k[m]$ only the imaginary part $f^{(\mathrm{I})}_{k,n}$. That also means that solving (7) leads only to $\boldsymbol{f}^{(\mathrm{R})}_{k,\mathrm{o}}$, while solving for $\hat{b}_k[m]$ and $b_k[m-\nu]$ leads to the same result for $\boldsymbol{w}_{k,\mathrm{o}}$ and only to $\boldsymbol{f}^{(\mathrm{I})}_{k,\mathrm{o}}$. However, it can be proven that in this case $\boldsymbol{f}^{(\mathrm{R})}_{k,\mathrm{o}} = \boldsymbol{f}^{(\mathrm{I})}_{k,\mathrm{o}}$.

We can write the vectors $\boldsymbol{y}^{(\mathrm{R})}_k[n]$ and $\boldsymbol{y}^{(\mathrm{I})}_k[n]$ in (5) and (6) as

$$\begin{aligned}\boldsymbol{y}^{(\mathrm{R})}_k[n] = \mathrm{Re}\left[\boldsymbol{y}_k[n]\right] \approx \boldsymbol{G}^{(\mathrm{R})}_k \boldsymbol{x}_k[n] + \boldsymbol{M}^{(\mathrm{R})}_k \boldsymbol{x}_{k-1}[n] + \\ \boldsymbol{N}^{(\mathrm{R})}_k \boldsymbol{x}_{k+1}[n] + \boldsymbol{\Gamma}^{(\mathrm{R})}_k \boldsymbol{\eta}^{(\mathrm{R})}[l] - \boldsymbol{\Gamma}^{(\mathrm{I})}_k \boldsymbol{\eta}^{(\mathrm{I})}[l],\end{aligned} \tag{8}$$

$$\begin{aligned}\boldsymbol{y}^{(\mathrm{I})}_k[n] = \mathrm{Im}\left[\boldsymbol{y}_k[n]\right] \approx \boldsymbol{G}^{(\mathrm{I})}_k \boldsymbol{x}_k[n] + \boldsymbol{M}^{(\mathrm{I})}_k \boldsymbol{x}_{k-1}[n] + \\ \boldsymbol{N}^{(\mathrm{I})}_k \boldsymbol{x}_{k+1}[n] + \boldsymbol{\Gamma}^{(\mathrm{R})}_k \boldsymbol{\eta}^{(\mathrm{I})}[l] + \boldsymbol{\Gamma}^{(\mathrm{I})}_k \boldsymbol{\eta}^{(\mathrm{R})}[l],\end{aligned} \tag{9}$$

where $\boldsymbol{x}_k[n]$ is obtained from (2) and (3) by shifting the j of each imaginary entry of $\boldsymbol{x}'_k[n]$ into the matrix $\boldsymbol{G}'_k$ what we define as $\boldsymbol{G}_k$. The same is done with $\boldsymbol{M}_k$ and $\boldsymbol{N}_k$. The dimensions do not change, but each second column of the matrices is multiplied by j, before either the real or imaginary part of the matrices is taken, as performed in (8) or (9).

As stated before, we consider that the complex input symbols are i.i.d. Additionally we assume that they have variance $\sigma_d^2 = \mathrm{E}\left[d[m]d^*[m]\right]$. We define the variance of the stationary AWGN as $\sigma_\eta^2 = \mathrm{E}[\eta[l]\eta^*[l]]$.

If we plug (5), (8) and (9) into (7) and apply the orthogonality principle, viz. $\mathrm{E}\left[\varepsilon^* \boldsymbol{y}'_k[n]\right] = \boldsymbol{0}_{2N+B+1}$, where $\varepsilon = \hat{a}_k[m] - a_k[m-\nu]$ and $\boldsymbol{y}'_k[n] = \left[\boldsymbol{y}^{(\mathrm{R}),T}_k[n], \boldsymbol{y}^{(\mathrm{I}),T}_k[n], \hat{\boldsymbol{x}}^T_k[n]\right]^T$, and use the definition $\boldsymbol{w}'_k = \left[\boldsymbol{w}^{(\mathrm{R}),\mathrm{T}}_k, \boldsymbol{w}^{(\mathrm{I}),\mathrm{T}}_k\right]^T \in \mathbb{R}^{2N}$, we end up with

$$\begin{bmatrix}\boldsymbol{w}'_{k,\mathrm{o}} \\ \boldsymbol{f}^{(\mathrm{R})}_{k,\mathrm{o}}\end{bmatrix} = \begin{bmatrix}\boldsymbol{H}_k \boldsymbol{H}^{\mathrm{T}}_k + \boldsymbol{F}_k \boldsymbol{F}^{\mathrm{T}}_k + \boldsymbol{R}_{\eta,k} & -\frac{\sigma_d}{\sqrt{2}} \boldsymbol{H}_k \boldsymbol{J}_\nu \\ -\frac{\sigma_d}{\sqrt{2}} \boldsymbol{J}^T_\nu \boldsymbol{H}^T_k & \frac{\sigma_d^2}{2} \boldsymbol{I}_{B+1}\end{bmatrix}^{-1} \begin{bmatrix}\frac{\sigma_d}{\sqrt{2}} \boldsymbol{H}_k \boldsymbol{e}_\nu \\ \boldsymbol{0}_{B+1}\end{bmatrix}, \tag{10}$$

with the matrix definitions

$$\boldsymbol{H}_k = \frac{\sigma_d}{\sqrt{2}} \begin{bmatrix}\boldsymbol{G}^{(\mathrm{R})}_k \\ \boldsymbol{G}^{(\mathrm{I})}_k\end{bmatrix}, \qquad \boldsymbol{F}_k = \frac{\sigma_d}{\sqrt{2}} \begin{bmatrix}\boldsymbol{M}^{(\mathrm{R})}_k & \boldsymbol{N}^{(\mathrm{R})}_k \\ \boldsymbol{M}^{(\mathrm{I})}_k & \boldsymbol{N}^{(\mathrm{I})}_k\end{bmatrix},$$

$$\boldsymbol{R}_{\eta,k} = \frac{\sigma_\eta^2}{2} \boldsymbol{\Gamma}'_k \boldsymbol{\Gamma}'^{,T}_k, \qquad \boldsymbol{\Gamma}'_k = \begin{bmatrix}\boldsymbol{\Gamma}^{(R)}_k & \boldsymbol{\Gamma}^{(I)}_k \\ \boldsymbol{\Gamma}^{(I)}_k & -\boldsymbol{\Gamma}^{(R)}_k\end{bmatrix},$$

and $\boldsymbol{J}_\nu$ is of size $(L+1) \times (B+1)$ and is defined as

$$\boldsymbol{J}_\nu = \begin{cases}\left[\boldsymbol{0}_{(\nu+1)\times(B+1)} \;\; \boldsymbol{I}_{B+1} \;\; \boldsymbol{0}_{(L-B-\nu-1)\times(B+1)}\right]^{\mathrm{T}}, & L-\nu > B+1, \\ \left[\boldsymbol{0}_{(\nu+1)\times(B+1)} \;\; \boldsymbol{I}_{B+1} \;\; \boldsymbol{0}_{(L-\nu)\times(B+\nu-L+1)}\right]^{\mathrm{T}}, & L-\nu < B+1, \\ \left[\boldsymbol{0}_{(\nu+1)\times(B+1)} \;\; \boldsymbol{I}_{B+1}\right]^{\mathrm{T}}, & L-\nu = B+1.\end{cases} \tag{11}$$

If perfect channel knowledge is available at the receiver, (10) gives the MMSE DFE solution in closed form.

IV. Simulation results

We have simulated the performance of the OQAM FBMC system applying the per-subcarrier DFE and the LE of [7] in a WiMAX framework. A sampling rate $M/T = 11.2$ MHz and a transmission bandwidth of 10 MHz have been considered. The input symbols have been modulated using 16-QAM.

We have considered two versions of the subchannel bandwidth, i.e. two different total numbers of subchannels in the FBMC. First, following the standard, we have used $M = 1024$ with a subchannel bandwidth of 10.94 kHz, where only 840 subchannels have been occupied with input symbols, the others had zero input. Then we have reduced the total number of subchannels to $M = 256$ with a subchannel bandwidth of 43.75 kHz, and occupied 210 subchannels. The data rate is the same for both configurations. But since the subchannels are wider for a lower M, the channel equalization is even more challenging. For that reason, we have also increased the length of the equalizers to evaluate its effectiveness. The motivation to use wider subchannels in an FBMC system is to benefit from a lower sensitivity to carrier frequency offset (CFO) and to Doppler effects, and a lower peak-to-average power ratio (PAPR).

As prototype filter we have employed a truncated version of a root raised cosine filter with $K = 4$ and roll-off factor $\rho = 0.5$, as this kind of filter is nearly Nyquist (nearly ISI-free) and with that roll-off factor only immediately adjacent subchannels have a significant overlap. A lower K would imply a higher interference between non-adjacent subchannels.

As channel model we have chosen the power delay profile of the Extended Typical Urban from 3GPP Long Term Evolution (LTE) in an static environment, i.e. without any Doppler effects.

Some simulation results in terms of uncoded bit error ratio (BER) as a function of E_b/N_0 are depicted in Fig. 6. In all the DFE simulations we have used $B = 1$, i.e. the feedback filter had length 2. We notice that there is a loss in performance, if M is reduced and N and B are kept unchanged. However, the DFE performs considerably better than the LE in high E_b/N_0 regimes. But if N is increased, a better performance is achieved, since a longer equalizer can compensate for higher frequency variations inside one subchannel coming along with the advantages listed above. It is worth mentioning that wider subcarriers are not desirable in CP-OFDM systems, as that would considerably reduce the spectral efficiency.

A. Complexity analysis

In [7] we have derived the increase in the computational overhead of an OQAM FBMC system in relation to a CP-OFDM system. We have considered an efficient implementation and have taken into account only the length of the LE, not its computation. Besides the FFT, also the polyphase filtering has to be accounted for in an FBMC system. Since there is only one equalizer per subchannel, the additional increase in complexity is a linear function of the number of subcarriers.

It turned out that, in the considered framework with an FBMC system the number of multiplications for each received symbol is in the order of five times that of an CP-OFDM system. The difference in the case of a DFE is that half of the length of the feedback filter has to be added to the length of the feedforward filter and then used as the total length of the equalizer, because of purely real (imaginary) feedback coefficients.

V. Conclusion

In this contribution we have investigated the problem of channel equalization in OQAM FBMC systems. We have derived a closed form solution for the per-subchannel DFE using the MMSE as design criterion. The analytical result holds only if no errors occur in the decision device.

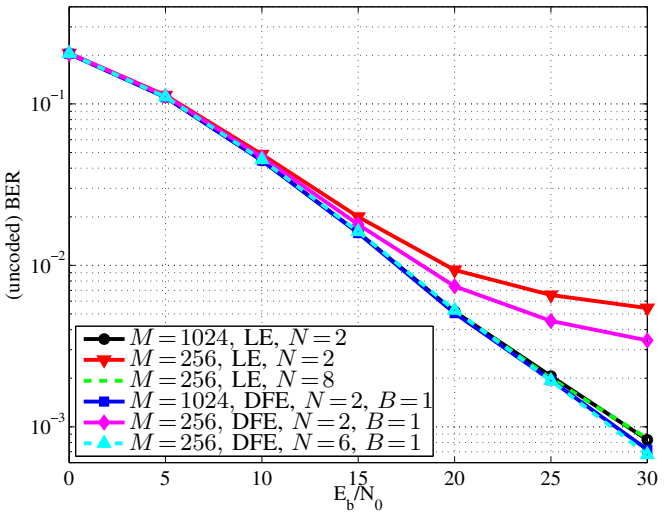

Fig. 6. Comparison between LE and DFE for different equalizer lengths and different number of subcarriers

Our results have shown that the DFE has a similar or improved performance in comparison to the LE for static channels. They have also illustrated that the increase in the subchannel bandwidth can be effectively compensated by the use of longer equalizers, i.e. without any performance loss.

The analytical solution has a high complexity in the calculation of the equalizer coefficients. In situations where Doppler effects are an issue an adaptive equalizer is necessary as we have proposed in [9]. The issue of channel estimation remains for future investigations.

Acknowledgment

This work was partially supported by the European Commission under the Project PHYDYAS (FP7-ICT-2007-1-211887).

References

[1] P. Siohan, C. Siclet, and N. Lacaille, "Analysis and design of ofdm/oqam systems based on filterbank theory," *IEEE Trans. Signal Processing*, vol. 50, no. 5, pp. 1170–1183, May 2002.

[2] J. G. Proakis, *Digital Communications*, 4th ed. New York, NY: McGraw-Hill, 2001.

[3] B. Hirosaki, "An analysis of automatic equalizers for orthogonally multiplexed QAM systems," *IEEE Trans. Commun.*, vol. COM-28, no. 1, pp. 73–83, January 1980.

[4] J. Louveaux, L. Vandendorpe, L. Cuvelier, F. Deryck, and O. van de Wiel, "Linear and decision-feedback MIMO equalization for transmultiplexer-based high bit rate transmission over copper wires," *Proc. Int. Zurich Seminar on Broadband Commun.*, pp. 177–184, Feb 1998.

[5] S. Nedic and N. Popovic, "Per-bin DFE for advanced OQAM-based multi-carrier wireless data transmission systems," *Proc. Int. Zurich Seminar on Broadband Commun.*, pp. 38–1–38–6, 2002.

[6] T. Ihalainen, T. H. Stitz, M. Rinne, and M. Renfors, "Channel equalization in filter bank based multicarrier modulation for wireless communications," *EURASIP J. Appl. Signal Process.*, vol. 2007, no. 1, pp. 140–140, 2007.

[7] D. S. Waldhauser, L. G. Baltar, and J. A. Nossek, "MMSE subcarrier equalization for filter bank based multicarrier systems," *Proc. IEEE SPAWC 2008*, pp. 525–529, July 2008.

[8] T. Karp and N. J. Fliege, "Computationally efficient realization of MDFT filter banks," *Proc. EUSIPCO '96*, vol. 2, pp. 1183–1186, September 1996.

[9] D. S. Waldhauser, L. G. Baltar, and J. A. Nossek, "Adaptive decision feedback equalization for filter bank based multicarrier systems," *Proc. IEEE ISCAS 2009*, May 2009.